

# Compton Scattering of $\gamma$ -Ray Vortex with Laguerre Gaussian Wave Function

Tomoyuki Maruyama,<sup>1,2</sup> Takehito Hayakawa,<sup>3,2</sup> and Toshitaka Kajino<sup>4,2,5</sup>

<sup>1</sup>*College of Bioresource Sciences, Nihon University, Fujisawa 252-8510, Japan*

<sup>2</sup>*National Astronomical Observatory of Japan,*

*2-21-1 Osawa, Mitaka, Tokyo 181-8588, Japan*

<sup>3</sup>*National Institute for Quantum and Radiological*

*Science and Technology, Tokai, Ibaraki 319-1106, Japan*

<sup>4</sup>*Beihang University, School of Physics and Nuclear Energy Engineering,*

*Int. Center for Big-Bang Cosmology and Element Genesis, Beijing 100191, China*

<sup>5</sup>*The University of Tokyo, Bunkyo-ku, Tokyo 113-0033, Japan*

In this work, we report calculation for Compton scattering of a  $\gamma$ -ray vortex with Laguerre Gaussian wave function on an electron in the framework of the relativistic quantum mechanics. We have found the following unexpected feature. The momentum of scattered photon distributes outside of the reaction plane determined by the incident photon and the scattered electron, and hence the energy of the scattered photon also distributes. This novel result indicates that one can identify a  $\gamma$ -ray vortex by measuring coincidentally the scattered angles of the electron and photon.

Photon vortices carrying orbital angular momentum [1] are interesting both from the fundamental research [2–4] and for applications [5–11]. Furthermore, it is suggested that the photon vortex can be created in astronomical system [12]. Recently, it has been proposed to generate  $\gamma$ -ray vortices in the MeV energy region using laser Compton scattering with laser vortex [13–15] and nonlinear laser Compton scattering with highly intense circularly polarized laser [16]. When  $\gamma$ -ray vortices are available in laboratory, they open a new frontier in nuclear and particle physics [16, 17]. However, there is no practical method to identify  $\gamma$ -ray vortices in the MeV energy region. Compton scattering is a dominant process of photons and atoms in the energy region from several hundred keV to several MeV. It is well known that the differential cross-section of Compton scattering of linearly polarized  $\gamma$ -rays depends on the angle between the scattering plane and the polarization plane. Thus, polarimeters based on Compton scattering have been used in nuclear physics [18] and  $\gamma$ -ray astronomy [19]. Thus, it is important to calculate the cross section of Compton scattering with  $\gamma$ -ray vortices.

We consider Compton scattering of a  $\gamma$ -ray vortex with a wave function of Laguerre Gaussian (LG) on an electron at rest. We also consider coincidence measurements of the scattered electron and photon. We set the system so that an initial photon propagates along the  $z$ -direction with the energy  $k$  and the electron is scattered in the  $zx$ -plane (see Fig. 1). The amplitude of Compton scattering in relativistic quantum mechanics [20] is given by

$$S_{if} = e^2 \int d^4x d^4y \bar{\psi}_f(x) \gamma^\mu S_F(x, y) \gamma^\nu \psi_i(y) \left[ A_f^{\mu*}(x) A_i^\nu(y) + A_i^\mu(x) A_f^{\nu*}(y) \right], \quad (1)$$

where  $e$  is the elementary charge,  $\psi_i$  and  $\psi_f$  are the initial and final electron wave functions, respectively,  $S_F$  is the electron propagator, and  $A_i \equiv (A_i^0, \mathbf{A}_i)$  and  $A_f \equiv (A_f^0, \mathbf{A}_f)$  are the initial and final photon fields, respectively. Though the momenta of photon vortices are under off-mass-shell condition, it is expected that the on-mass-shell condition is satisfied for observed photons. Therefore, we assume that the final photon wave function is the plane wave with the final photon momentum of  $q \equiv (|\mathbf{q}|, \mathbf{q}) = (|\mathbf{q}|, \mathbf{q}_T, q_z)$ .

We choose the Lorentz gauge and  $A_0 = 0$  for the photon field and write the electron and photon fields as

$$\psi(x) = \frac{1}{\sqrt{\Omega}} U(\mathbf{p}, s) e^{i\mathbf{p}\mathbf{r} - i\mathbf{E}_p \mathbf{t}}, \quad \mathbf{A}_i(\mathbf{r}) = \frac{\boldsymbol{\epsilon}_i(h_i)}{\sqrt{2k}} u(\mathbf{r}) e^{-ikt}, \quad \mathbf{A}_f(\mathbf{r}) = \frac{\boldsymbol{\epsilon}_f(h_f)}{\sqrt{2|\mathbf{q}|\Omega}} e^{i\mathbf{q}\mathbf{r} - i|\mathbf{q}|\mathbf{t}}, \quad (2)$$

where  $\Omega$  is the volume of the system,  $U(\mathbf{p}, s)$  is the Dirac spinor of an electron with the momentum  $\mathbf{p}$  and the spin  $s$ ,  $k$  is the energy of the initial photon,  $h_{i(f)}$  indicates the helicity of the initial (final) photon, and the polarization vector satisfies  $\boldsymbol{\epsilon}_f \cdot \mathbf{q} = 0$  and  $\boldsymbol{\epsilon}_f \cdot \boldsymbol{\epsilon}_f = 1$ . We write the initial and final momenta of the electron as  $p_i = (E_i, \mathbf{p}_i)$  and  $p_f = (E_f, \mathbf{p}_f)$ , respectively. The

scattering amplitude is rewritten as

$$S_{if} = \frac{e^2}{2\sqrt{k_i^0|\mathbf{q}|\Omega}} \bar{U}(\mathbf{p}_f, s_f) [\not{\epsilon}_f S_F(p_f + q) \not{\epsilon}_i + \not{\epsilon}_i S_F(p_i - q) \not{\epsilon}_f] U(\mathbf{p}_i, s_i) \times \tilde{u}(\mathbf{p}_f + \mathbf{q} - \mathbf{p}_i) (2\pi) \delta(E_f + |\mathbf{q}| - E_i - k) \quad (3)$$

with  $\epsilon_{i,f} = (0, \boldsymbol{\epsilon}_{i,f})$  and

$$S_F(p) = \frac{\not{p} + m}{p^2 + m^2 + i\delta}, \quad \tilde{u}(\mathbf{k}) = \int d\mathbf{r} e^{-i\mathbf{k}\cdot\mathbf{r}} u(\mathbf{r}). \quad (4)$$

Then, the cross-section is given by

$$d\sigma = \frac{e^4}{4kE_i} W_{if} |\tilde{u}(\mathbf{p}_f + \mathbf{q} - \mathbf{p}_i)|^2 (2\pi) \delta(E_f + |\mathbf{q}| - E_i - k) \frac{d\mathbf{q}}{(2\pi)^3 |\mathbf{q}|} \frac{d\mathbf{p}_f}{(2\pi)^3 E_f} \quad (5)$$

with

$$W_{if} = E_i E_f |\bar{U}(\mathbf{p}_f, s_f) [\not{\epsilon}_f(h_k) S_F(p_f + q) \not{\epsilon}_i + \not{\epsilon}_i S_F(p_i - q) \not{\epsilon}_f(h_k)] U(\mathbf{p}_i, s_i)|^2. \quad (6)$$

We assume that the initial electron is at rest, that the initial photon is parallel to  $z$ -direction, and that the final photon polarization is not observed. Then, we substitute  $p_i = (m, 0, 0, 0)$  and  $\epsilon_i(h_i) = (1, ih_i, 0)/\sqrt{2}$  with  $h_i = \pm 1$ . We average the spin of the initial electron and sum over the spin of the final electron and the polarization of the final photon. In addition, we rewrite  $p_f = (E_p, \mathbf{p}_e) = (E_p, \mathbf{p}_T, p_z)$ . As the result, the cross-section is written as

$$d\sigma = \frac{\alpha^2 w_0^2}{8\pi^3 m k |\mathbf{q}| E_p} \bar{W}_{if} |\tilde{u}(\mathbf{p} + \mathbf{q})|^2 \delta(E_p + |\mathbf{q}| - m - k) d\mathbf{q} d\mathbf{p}, \quad (7)$$

with

$$\begin{aligned} \bar{W}_{if} &= \frac{1}{2} \sum_{s_i, s_f, h_f} W_{if} \\ &= \frac{1}{8} \sum_{h_k} \text{Tr} \left\{ (\not{p}_f + m) \left[ \frac{(2p_f \cdot \epsilon_f(h_k) - \not{k}_f \not{\epsilon}_f(h_k)) \not{\epsilon}_i}{2p_f \cdot k_f} - \frac{\not{\epsilon}_i (\not{\epsilon}_f(h_k) \not{k}_f + 2p_i \cdot \epsilon_f(h_k))}{2p_i \cdot k_f} \right] \right. \\ &\quad \left. \times (\not{p}_i + m) \left[ \frac{\not{\epsilon}_i^* (2p_f \cdot \epsilon_f - \not{\epsilon}_f \not{k}_f)}{2p_f \cdot k_f} - \frac{(\not{k}_f \not{\epsilon}_f + 2p_i \cdot \epsilon_f) \not{\epsilon}_i^*}{2p_i \cdot k_f} \right] \right\} \\ &= \frac{1}{2} \left\{ \frac{mq_z^2}{|\mathbf{q}|(p_f \cdot q)} + \frac{mk}{(p_f \cdot q)^2} \left[ |\mathbf{p}|^2 - \frac{(\mathbf{p} \cdot \mathbf{q})^2}{|\mathbf{q}|^2} \right] \right. \\ &\quad \left. + \frac{E_p |\mathbf{q}| - p_z q_z}{m|\mathbf{q}|} + \frac{p_z}{(p_f \cdot q)} \left[ \frac{q_z (\mathbf{p} \cdot \mathbf{q})}{|\mathbf{q}|^2} - p_z \right] \right\}. \quad (8) \end{aligned}$$

Note that these cross-sections are independent of the initial photon helicity  $h_i$ .

In this work, we consider the LG wave [1] for the initial photon which is written as

$$u(\mathbf{r}) = \sqrt{\frac{2}{\pi R_z}} \frac{1}{w(z)} G \left[ |L|, p, \frac{r}{w(z)} \right] \exp \left\{ i \left[ L\phi + kz + \frac{zr^2}{z_R w^2(z)} - (2p + |L| + 1)\theta_G \right] \right\} \quad (9)$$

with

$$G[|L|, p, x] = \sqrt{\frac{p!}{\pi(|L| + p)!}} \left(\frac{x}{\sqrt{2}}\right)^{|L|} e^{-x^2/4} \mathcal{L}_p^{|L|} \left(\frac{x^2}{2}\right),$$

$$\theta_G = \tan^{-1} \left(\frac{z}{z_R}\right), \quad w(z) = w_0 \sqrt{1 + z^2/z_R^2}, \quad z_R = kw_0^2/2. \quad (10)$$

where  $L$  is an integer indicating the orbital angular momentum of the initial photon,  $\mathcal{L}_p^{|L|}$  is the associated Laguerre function,  $R_z$  is the size of the system along the  $z$ -direction, and  $w_0$  is the waist radius at  $z = 0$ . The Fourier transformation of  $u(\mathbf{r})$  becomes

$$\tilde{u}(\mathbf{Q}) = \sqrt{\frac{(2\pi)^3}{R_z}} e^{i(p+|L|/2)\pi} e^{iL\phi_q} w_0 G[|L|, p; w_0 Q_T] \delta \left( Q_z + \frac{Q_T^2}{2k} - k \right) \quad (11)$$

with  $Q_T \equiv \sqrt{Q_x^2 + Q_y^2}$  and  $\phi_q$  being the azimuthal angle of the momentum  $\mathbf{Q}$  along  $z$ -axis.

Here, we consider coincident measurements of the scattered photon and electron. When the initial photon is the plane wave with momentum  $(0, 0, k)$ , the final electron momentum is  $\mathbf{p}_e/p_e = (-\sin \theta_e, 0, \cos \theta_e)$  with  $p_e = 2mk(k+m) \cos \theta_e / [(k+m)^2 - k^2 \cos^2 \theta_e]$  and the final photon momentum is  $\mathbf{q} = \mathbf{q}_0 = |\mathbf{q}_0|(\sin \phi_0, 0, \cos \phi_0) = (p_e \sin \theta_e, 0, k - p_e \cos \theta_e)$ . In contrast, when the incident photon is the LG wave, the final photon momentum distributes, while the initial photon momentum is given by  $\mathbf{Q} = \mathbf{p}_e + \mathbf{q}$ , thereby satisfying the relation  $p_z + q_z + (\mathbf{p}_T + \mathbf{q}_T)^2/2k - k = 0$  [see Eq. (11)]. To illustrate the final photon momentum distribution, we take  $y$ -direction to be a new principal axis and write the final photon momentum as  $\mathbf{q} = |\mathbf{q}|(\cos \theta_y \sin \phi_y, \sin \theta_y, \cos \theta_y \cos \phi_y)$  as shown in Fig. 1. Combining Eqs. (7) and (11), we obtain the cross-section for the incident photon of LG wave. By integrating the cross-section over  $|\mathbf{q}|$  and  $\phi_y$  for a fixed electron momentum, the cross-section is written as

$$\frac{d^4\sigma}{d\mathbf{p}_e^3 d\sin \theta_y} = \frac{\alpha^2 w_0^2 |\mathbf{q}|}{4\pi m E_p |(k - q_z)q_x - q_z |\mathbf{p}_T||} \bar{W}_{if} [G(L, p; w_0 |\mathbf{p}_T + \mathbf{q}_T|)]^2 \quad (12)$$

with  $|\mathbf{q}| = k + m - E_p$ . An important consideration in measurements is the divergence angle of the incident photon, which is determined by the photon energy  $k$  and the waist radius  $w_0$ . We take the incident photon energy to be  $k = 500$  keV, where Compton scattering dominates. Although  $w_0$  is a free parameter in the present calculation, it is determined by the generation mechanism of  $\gamma$ -ray vortices in the framework of the quantum mechanics. However, to our knowledge, there is no theoretical prediction. Thus, we take  $w_0$  to be 25 pm that is approximately ten times of the wave length of the present incident photon (2.48 pm) in the following discussion.

We find two unexpected features. First, the differential cross-sections have finite values out of the  $zx$ -plane. Figure 2(a) shows the angles of the scattered photons which give the finite cross-sections justifying the relation  $p_z + q_z + (\mathbf{p}_T + \mathbf{q}_T)^2/2k - k = 0$  when  $\cos \theta_e = 0.95$ . The

results exhibit that the distributions of the cross-sections are perpendicular to the horizontal axis at  $\theta_y = 0$ , clearly implying that the strengths of the cross-sections distribute out of the  $zx$ -plane. Second, the energy of the scattered photon is shifted from that of the standard Compton scattering. In addition, the energy shift correlates with the spatial shift from the  $zx$ -plane. The lower panel [Fig. 2(b)] shows the cross-sections for the LG waves with  $L = 1$  and  $p = 0$  as a function of the energy shift  $\Delta E = |\mathbf{q}| - |\mathbf{q}_0|$  and the scattered angle to  $y$ -axis,  $\theta_y$ . It should be emphasized that the strengths are exactly zero at  $\phi_y = 0$  and  $\Delta E = 0$ , at which the strength appears in the standard Compton scattering. This corresponds to the fact that the amplitude of the LG wave function is zero along the beam line when  $L \neq 0$ .

Let us discuss the result quantitatively. We show the differential cross-sections at  $\cos \theta_e = 0.95$  when  $L = 1$  and  $p = 0$  (a,b),  $L = 1$  and  $p = 1$  (c,d) and  $L = 2$  and  $p = 0$  (e,f) in Fig. 3. The left panels (a,c,e) present the angular dependence of the scattered photons. It is again confirmed the result that the strengths are exactly zero at  $\phi_y = 0$  and  $\Delta E = 0$  (see the solid lines), at which the strength appears in the standard Compton scattering. The position of the peak depends on  $L$ . In the case of (a), the peak with  $\Delta E = 0$  is located at  $\phi_y/\pi = 0.015$ . As  $L$  increases, the peak position shifts toward a larger polar angle [see Figs. 3(e)], which also corresponds to the shape of the photon wave function represented by the Laguerre function  $\mathcal{L}_p^L$ . Furthermore, the number of the peaks correlates with the node,  $p$ . In the case of (c), there are two peaks, which originates from the fact that the photon wave function has a node in the transverse direction for  $p = 1$ . These results indicate that, by measuring the angles of the scattered photon and electron, one can identify the angular momentum and the node of the LG wave for incident photon.

The right panels (b,d,f) present the expected energy spectra of the scattered photons. In the case of the standard Compton scattering, the energy is uniquely determined (see long dashed-lines); however, the energy of  $\gamma$ -ray vortices spreads. This result indicates another method to identify  $\gamma$ -ray vortex in the measurements: the energy and angle of the scattered photon coincidentally with the angle of the scattered electron. Finally, we point out that the cross-sections are dependent on the scattered electron angle, though we show only the results at  $\cos \theta_e = 0.95$ . As  $\theta_e$  decreases, the energy distributions become broader while the  $\theta_y$  distributions become narrower.

The  $\gamma$ -ray vortex is expected to be generated by laboratory experiments in the near future. In the present study, we study the Compton scattering with the gamma-ray vortex with the LG wave function, thereby find two unexpected features. First, the differential cross-sections have finite values out of the  $zx$ -plane. Second, the energy of the scattered photon shifts from that of the standard Compton scattering. These results indicate that Compton scattering with

$\gamma$ -ray vortices is useful to identify the nature of the photon vortices, the node  $p$  and the angular momentum  $L$ , when the final electron and photon are coincidentally measured.

This work was supported by Grants-in-Aid for Scientific Research of JSPS ( 15H03665, 16K05360, 17K05459.).

- 
- [1] L. Allen, *et al.*, Phys. Rev. A **45**, 8185 (1992).
  - [2] M. Babiker, W. L. Power, and L. Allen, Phys. Rev. Lett. **73**, 1239 (1994).
  - [3] A. Alexandrescu, D. Cojoc, and E. I. DiFabrizio, Phys. Rev. Lett. **96**, 243001 (2006).
  - [4] A. Picon, *et al.*, New J. Phys. **12**, 083053 (2010).
  - [5] A. M. Yao and M. J. Padgett, Adv. Opt. Photon. **3**, 161 (2011).
  - [6] X. Cai, *et al.*, Science. **338**, 363 (2012).
  - [7] J. Wang, *et al.*, Nat. Phot. **6**, 488 (2012).
  - [8] M. P. J. Lavery, *et al.*, Science **341**, 537 (2013).
  - [9] K. Toyoda, *et al.*, Phys. Rev. Lett. **110**, 143603 (2013).
  - [10] A. Afanasev, C. E. Carlson, and A. Mukherjee, Phys. Rev. A. **88** 033841 (2013).
  - [11] N. Bozinovic, *et al.*, Science **340**, 1545 (2013).
  - [12] F. Tamburini, Nat. Phys. **7**, 195 (2011).
  - [13] U. D. Jentschura and V. G. Serbo, Phys. Rev. Lett. **106**, 013001 (2011).
  - [14] U. D. Jentschura and V. G. Serbo, Eur. Phys. J. C **71**, 1571 (2011).
  - [15] V. Petrillo, *et al.*, Phys. Rev. Lett. **117**, 123903 (2016).
  - [16] Y. Taira, T. Hayakawa, and M. Katoh, Sci. Rep. **7**, 5018 (2017).
  - [17] I. P. Ivanov, Phys. Rev. D **83**, 093001 (2011).
  - [18] P. M. Jones, *et al.*, Nucl. Instr. Methods Phys. Res. A **362**, 556 (1995).
  - [19] F. Lei, A. J. Deam, and G. L. Hills, Spac. Sci. Rev. **82**, 309 (1997).
  - [20] S. D. Bjorken and S. D. Drell, "Relativistic Quantum Fields (Dover Books on Physics)", Dover Publications (November 25, 2014)

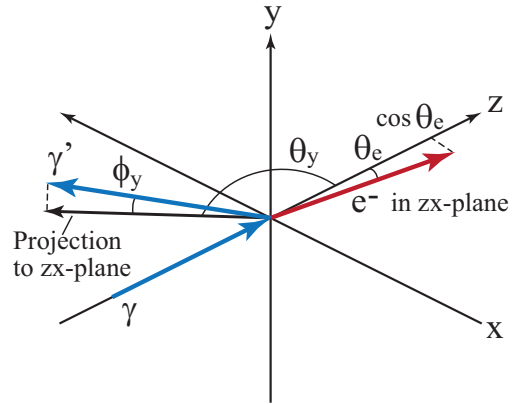


FIG. 1. Coordinate system used in the calculation.  $\gamma$  and  $\gamma'$  denote the initial and final photons, respectively. The electron as  $e^-$  is scattered in the  $zx$ -plane.

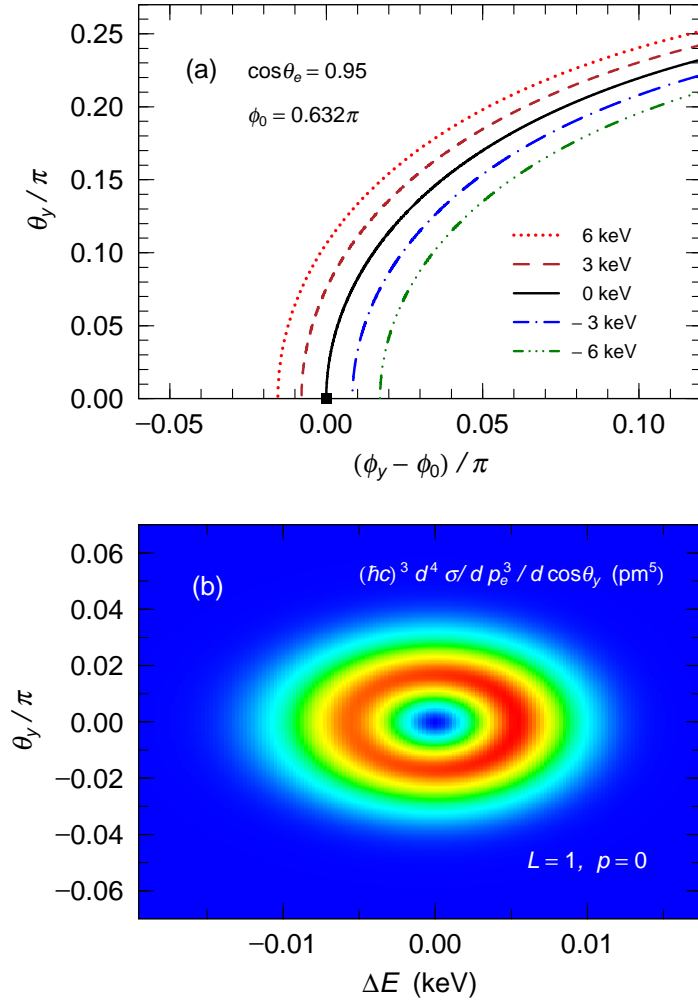


FIG. 2. Upper panel (a): the directions of the scattered photons at the fixed momenta of the final electrons, when  $\cos\theta_e = 0.95$ . The dotted, dashed, solid, dot-dashed, and dpt-dot-dashed lines represent the results when  $\Delta E = 6$  keV, 3 keV, 0 keV,  $-3$  keV, and  $-6$  keV, respectively. Lower panel (b): the contour plots of the differential cross-section of Compton scattering integrated over the azimuthal angle  $\phi_y$  when  $L = 1$ ,  $p = 0$ , and  $\cos\theta_e = 0.95$ . The horizontal axis shows the energy difference  $\Delta E$ , and the vertical axis shows the polar angle along the  $y$ -axis.



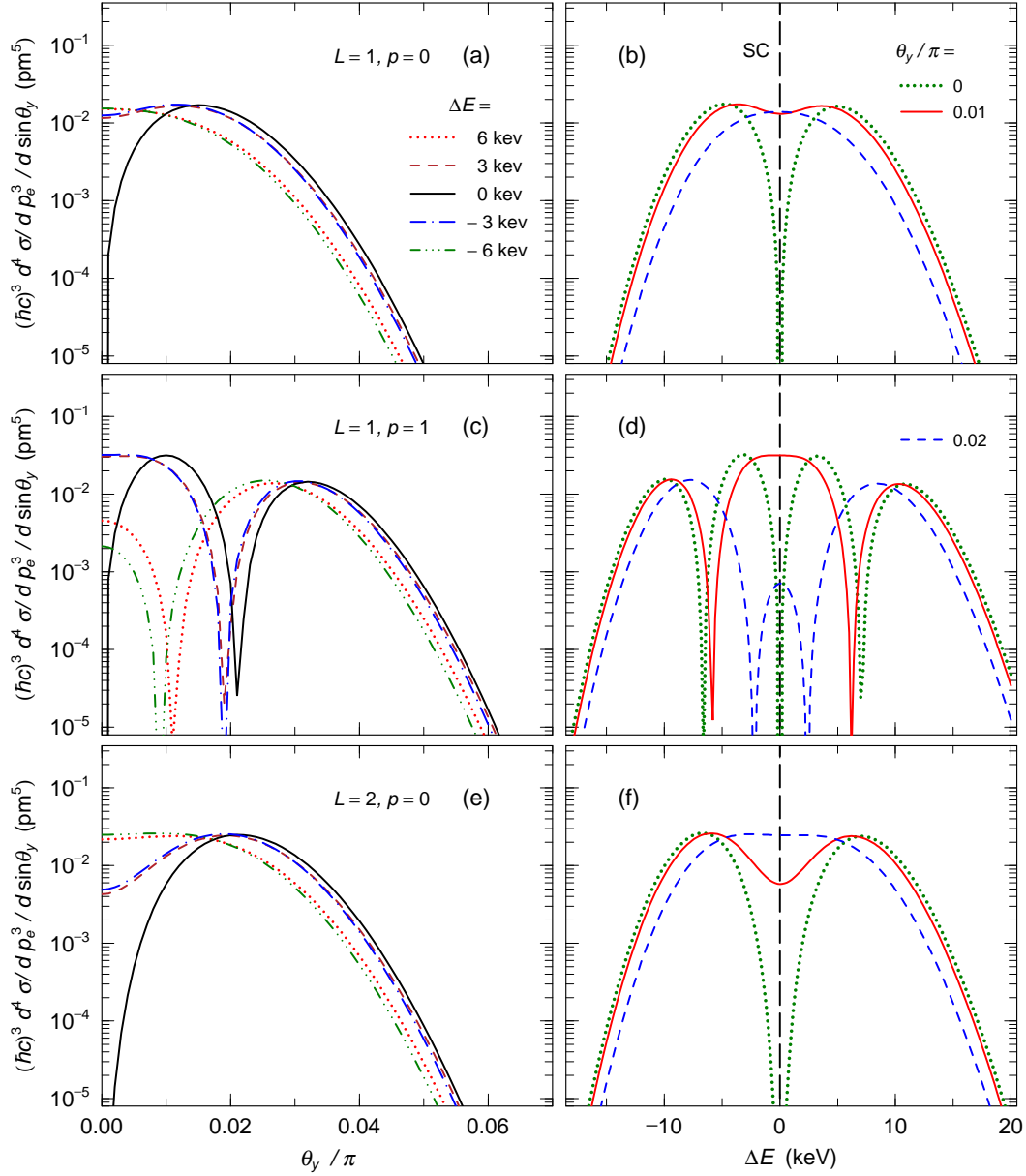


FIG. 3. The differential cross-section of Compton scattering when  $\cos\theta_e = 0.95$ . The left panels show the  $\theta_y$  dependence when  $L = 1, p = 0$  (a),  $L = 1, p = 1$  (c), and  $L = 2, p = 0$ . The dotted, dashed, solid, dot-dashed, and dpt-dot-dashed lines represent the results when  $\Delta E = 10$  keV, 5 keV, 0 keV,  $-5$  keV, and  $-10$  keV, respectively. The right panels show its energy spectra of the scattered photons, when  $L = 1, p = 0$  (b),  $L = 1, p = 1$  (d), and  $L = 2, p = 0$  (f). The dotted, solid, and dashed lines represent the results when  $\theta_y/\pi = 0, 0.01$ , and  $0.02$ , respectively. The long dashed lines indicate the results in the standard Compton (SC) scattering.